Carbohydrate Polymers 80 (2010) 350–359

Contents lists available at ScienceDirect

Carbohydrate Polymers

journal homepage: www.elsevier.com/locate/carbpol

Preparation and properties of a novel biodegradable ethyl cellulose grafting copolymer with poly(*p*-dioxanone) side-chains

Jiang Zhu, Xue-Ting Dong, Xiu-Li Wang *, Yu-Zhong Wang

Center for Degradable and Flame-Retardant Polymeric Materials (ERCEPM-MoE), College of Chemistry, State Key Laboratory of Polymer Materials Engineering, Sichuan University, 29 Wangjiang Road, Chengdu 610064, China

ARTICLE INFO

Article history:
Received 10 October 2009
Received in revised form 11 November 2009
Accepted 18 November 2009
Available online 22 November 2009

Keywords:
Ethyl cellulose
Poly(*p*-dioxanone)
Graft copolymer
Thermal properties
Crystalline behaviors
In vitro degradation

ABSTRACT

A novel biodegradable ethyl cellulose (EC) grafting copolymer with poly(*p*-dioxanone) side-chains were successfully synthesized via ring-opening polymerization (ROP) of *p*-dioxanone (PDO) with a tin 2-ethylhexanoate ($Sn(Oct)_2$) catalyst in bulk at 120 °C. By adjusting the molar ratios of PDO monomer to EC, the different side-chain lengths can be introduced onto EC backbone. The thermal properties and crystalline behaviors of EC-*g*-PPDO copolymers (EGPs) were different from those of linear PPDO. Furthermore, the in vitro degradation rate of EGPs was faster than the linear PPDO counterpart, and the degradability of grafting copolymers was decreased with the increase of the crystallinity of PPDO side-chains.

1. Introduction

Recently, aliphatic polyesters have attracted great interest of researchers owing to their excellent biodegradability, biocompatibility, and permeability (Gan, Yu, Zhong, Liang, & Jing, 1999). These materials such as poly(glycolic acid) (PGA), poly(ε-caprolactone) (PCL), poly(L-lactide) (PLLA), and their copolymers were usually used as sutures, drug delivery carrier, and temporary tissue scaffolds (Bisht, Deng, Gross, Kaplan, & Swift, 1998; Brostrom, Boss, & Chronakis, 2004; Ho et al., 2006; Ko & Lin, 2001; Li, Danielson, Alexander, & Tuan, 2003; Meng, Zheng, Zhang, Li, & Liang, 2006; O'Keefe et al., 2001; Wang, Bronich, Kabanov, Rauh, & Roovers, 2005; Wang & Hsiue, 2005). As one of important aliphatic polyesters, poly(1,4-dioxan-2-one) (PPDO) owns interesting properties such as the ultimate biodegradability and the good flexibility due to the coexistence of ester bonds and ether bonds in its backbone, which has already been used as monofilament sutures, bone and tissue fixation devices, or drug delivery systems (Libiszowski et al., 2004; Yang, Wang, & Wang, 2002).

The ring-opening polymerization (ROP) is a popular method for producing biodegradable polyesters including PPDO with covalent multivalent metal (Al, Sn(II), Sn(IV), Zn, etc.) alkoxides or carboxylates as catalysts, such as $Sn(Oct)_2$ or $Al(Et)_3$ (Haruo, Mitsuhiro, Masumi, Takeshi, & Yutaka, 2000; Kricheldorf & Damrau, 1998; Nishida, Yamashita, Endo, & Tokiwa, 2000; Raquez, Degee, Narayan, & Dubois, 2001; Raquez, Narayan, & Dubois, 2000; Wang, Qiu, & Gu, 1998). As an efficient catalyst for the ROP of lactones, tin 2-ethylhexanoate ($Sn(Oct)_2$) has unique advantages of a low biologic toxicity, controlled molecular weight, and narrow distribution (Deng et al., 2005; Kowalski et al., 2005; Odile, Blanca, & Didier, 2004; Rieger et al., 2005). Nishida et al. clarified the equilibrium polymerization behavior of PDO with $Sn(Oct)_2$ as a catalyst in bulk (Nishida et al., 2000). The copolymerizations of 1,4-dioxan-2-one (PDO) with trimethylene carbonate (TMC) in the presence of $Sn(Oct)_2$ had been achieved by Wang et al. (1998).

However, there are some limitations which prevent PPDO from the wide applications, such as the high cost and the low degradation rate (Chen et al., 2007). Graft copolymerization can provide an efficacious method not only for providing functionality to the resulting polymers, but for regulating polymer properties. Because the ROP of lactone may be initialized easily by the hydroxyl group when $Sn(Oct)_2$ was used, many researchers have utilized this method to prepare graft copolymers based on PPDO and other hydrophilic polymers (Chen, Zhou, Wang, Wang, & Yang, 2006; Liu et al., 2008; Wang, Yang, Wang, Zhou, & Jin, 2004).

As one of the widely applied derivatives of cellulose, which comes from the inexhaustible natural polymeric material in the world, ethyl cellulose (EC) displays interesting structures and properties as extensive linearity, chain stiffness, good solubility in organic solvents, good biocompatibility, high mechanical inten-

* Corresponding author. Tel./fax: +86 28 85410755.
E-mail addresses: xiuliwang1@163.com (X.-L. Wang), yzwang@scu.edu.cn (Y.-Z. Wang).

0144-8617/$ - see front matter © 2009 Elsevier Ltd. All rights reserved.
doi:10.1016/j.carbpol.2009.11.027

sity, stability, and nontoxicity (Shen, Yu, & Huang, 2005). Considerable attention has been paid to the chemical modification of cellulose and ethyl cellulose. For instance, Hult et al. completed the grafting of cellulose with poly(ε-caprolactone) and poly(L-lactide) via ROP (Lonnberg et al., 2006). Huang et al. synthesized the graft copolymers of ethyl cellulose with poly(methyl methacrylate) by atom transfer radical polymerization (Shen & Huang, 2004). EC-*g*-PCL-*b*-PLLA graft-block copolymers was prepared by ROP of lactide initiated by a hydroxyl-terminated EC-*g*-PCL macroinitiator in the presence of $Sn(Oct)_2$ in bulk (Yuan, Yuan, Zhang, & Xie, 2007). However, there are few reports about graft copolymerization of PPDO with cellulose and its derivatives (Zhu, Wang, Wang, Li, & Wang, 2009).

In this work, a novel graft copolymer based on the EC backbone was synthesized by ROP in bulk in the presence of ($Sn(Oct)_2$). Grafting PPDO onto EC backbone will helpful for lowering the cost of PPDO and ameliorating the discontinuous degradation of PPDO. The chemical structure of grafting copolymers was characterized by IR and NMR. The thermal properties of the obtained copolymers were investigated by DSC and TG. The crystalline behaviors of the grafting polymers were observed by wide-angle X-ray diffraction (WAXD) and polarizing optical microscope (POM). Furthermore, the in vitro degradation of the copolymer was investigated in a phosphate buffered saline solution. By controlling the numbers and length of PPDO chains, the properties of the graft copolymer can be modulated. To the best of our knowledge, this is the first paper on the synthesis and characterization of EC-*g*-PPDO (EGP) copolymer.

2. Experimental

2.1. Materials

Ethyl cellulose (EC) (M_n = 53,809; the degree of ethyl substitution is 2.17) was obtained from Shanghai Chemical Reagent Co., Ltd. and was dried at 70 °C for 48 h under vacuum before use. *p*-Dioxanone (PDO) that was supplied by the Pilot Plant of the Center for Degradable and Flame-Retardant Polymeric Materials (Chengdu, China) was dried over CaH_2 for 48 h, and distilled twice under reduced pressure immediately before use. Stannous octoate ($Sn(Oct)_2$) was obtained from Sigma (USA) and was used without any further purification. After dilution with dry toluene, $Sn(Oct)_2$ solution was stored in a glass ampule under argon. Toluene was received from the Hehong Chemical Reagent Factory (Chengdu, China) and was dried by refluxing over a sodium/benzophenone complex and distilled just before use. Other solvent with AP grade were purchased from Bodi chemical Factory (Tianjin, China) and used without further purification.

2.2. Synthesis of EGP copolymer

A typical procedure to synthesize EGP was as followed: EC (2.00 g; 7.70 mmol in anhydroglucose unit) was charged into a stringently dried 50 mL flask and purged three times with dry nitrogen. Then PDO monomer (3.92 g; 19.22 mmol) was added by a syringe. Consequently, the flask was put into a preheated oil bath (T = 100 °C) for about 30 min to obtain a clear homogenous melt system. And then ($Sn(Oct)_2$) (0.24 mL; 0.05 mmol) was syringed under nitrogen at 120 °C and the reaction was allowed to proceed at the same temperature for 1 h defined as a reaction time of grafting. After quickly cooling to 0 °C, the crude resultants were dissolved in phenol/tetrachloroethane (1:1 v/v) and precipitated by anhydrous methanol. Then the deposits were extracted with acetone in a Soxhlet apparatus for 48 h to remove the homopolymer. Finally, the products were dried at 60 °C in vacuum to constant weight.

2.3. Characterization of EGP copolymers

The chemical structure of EGP was characterized by one- and two- dimensional NMR spectroscopy. One-dimensional NMR spectra were obtained through the ^{13}C and ^{1}H nuclei, and were conducted by using an Avance Bruke-II 600 NMR instrument. The processing conditions were as follows: solvent, $CDCl_3$; internal standard, tetramethylsilane (TMS). The detailed information on the direct C–H connectivity in the structure of CDA-*g*-PPDO was obtained by two-dimensional hetero-nuclear multiple quantum coherence (HSQC) spectroscopy. The processing parameters were as follow: solvent, $CDCl_3$; internal standard, tetramethylsilane (TMS); solute concentration, 60 mg mL^{-1}; scan frequency, 600 MHz for ^{13}C and 150 MHz for ^{1}H.

Molecular weight distribution of graft copolymers were determined by gel permeation chromatography (GPC), on a system equipped with a Waters 1515 pump, a 717 automatic injector, and a 2414 differential refractometer detector. The measurement was performed by using chloroform ($CHCl_3$) as eluant at flow rate of 1.0 mL min^{-1}. The concentration of test samples was 15 mg mL^{-1} and the quantity of injection was 0.5 mL. Monodispersed polystyrene was used as the standard for the calibration curve.

Differential scanning calorimetry (DSC) was carried out with a TA instrument DSC Q200 apparatus. The measurements were carried out at a scanning rate of 10 °C min^{-1} in a sealed aluminium pan under nitrogen atmosphere with the calibration of an indium standard. At first the samples were kept 5 min at 120 °C to eliminate the thermal history, and then cooled from 120 to −30 °C as the first cooling run. At last the samples were again heated from −30 to 150 °C for the second heating scan. The glass temperature (T_g) and the melting temperature (T_m) were acquired from the thermograms.

The thermal stability of graft copolymers and EC were performed by a NETZSCH device TG 209 F1. The examinations were executed at a heating rate of 10 °C min^{-1} in crucibles under the nitrogen atmosphere from 40 to 600 °C.

Crystal morphology of the graft copolymer and pure PPDO were performed by a Nikon ECLIPSE LV100POL polarizing optical microscope (POM) equipped with an INSTEC HCS621V hot-stage device. The spherulitic shape was observed in the following procedure: small pieces of samples were melted between slides and cooled to the room temperature. Before the crystallization process, the specimens were heated to 120 °C, then maintained for 3 min, and subsequently quickly cooled to 40 °C under the regulation of the hot stage.

Wide-angle X-ray diffraction (WAXD) patterns of powder samples (EC and EC-*g*-PPDO) were obtained on a DX-1000 X-ray diffractometer with a Cu Kα radiation source (40 kV, 25 mA). Samples were exposed at a scanning rate of 2θ = 2–70°.

The in vitro degradation tests were carried out in a phosphate buffer solution with pH 7.4 at 37 °C for 30 days. Films were cut into 20 × 10 mm^2 slabs with a thickness of 0.3 mm. The samples were prepared by compression molding at 110 °C, followed by rapid cooling at room temperature. The specimens were stored in vacuum at 30 °C for 48 h. The degradation behaviors of PPDO and copolymers were investigated by detecting weight loss of specimens, which were washed with the distilled water and dried in vacuum at room temperature to a constant weight at given time intervals.

3. Results and discussion

3.1. Characterization of EGP copolymers

Because EC had good solubility in PDO monomer, the homogeneous ring-opening graft copolymerization of PDO with EC could be carried out successfully without any solvent in the presence of $Sn(Oct)_2$. To clear the microstructure of EGP resultant, NMR spectroscopy was used to determine the structure parameters of the graft

copolymer. Firstly, we got the detailed information of the peaks of all carbon species in EGP copolymer from ^{13}C NMR (exhibited in Fig. 1A), which has a spectral range wide enough to assign easily every peak in the spectrum compared to ^{1}H NMR (see in Fig. 1B). Finally, the direct C–H connectivity between each carbon and the proton attached directly to it was validated by the HSQC spectrum. Fig. 1C exemplifies the typical HSQC spectrum of EGP sample. The longitudinal axis of the spectrum belongs to the chemical shift of the one-dimensional ^{13}C NMR spectrum, and the transverse axis corresponds to that of the one-dimensional ^{1}H NMR spectrum.

From Fig. 1, in contrast with the original substrate, the new distinct peaks that appeared at 62.7–69.2 and 171.0 ppm were ascribed to the alkyl carbon species and the carbonyl carbon of PPDO side-chains apart. The carbons of the backbone of EC appeared at 100.1, 73.5, 81.1, and 61.6 ppm corresponding to C_1, $C_{2,3,5}$, C_4, and C_6 in anhydrous glucose unit (AGU), respectively. Moreover, the chemical shift at 64.7 ppm designated for the $-CH_2$ carbon (C_e) and the shift at 15.2 ppm assigned to the $-CH_3$ carbon (C_d) for the ethoxy group in the native EC. These data indicated doubtlessly the grafting of PPDO onto EC backbone.

On the other hand, in the proton species of the resulting graft copolymer based on ^{1}H NMR (see in Fig. 1B), one can see clearly that EGP gave the new strong signals at 4.18, 3.80, and 4.22 ppm assigned to the internal methylene protons (H_a, H_b, H_c) of PPDO side-chains and the signals at 4.21, 3.76, and 3.70 ppm corresponding to the terminal methylene protons ($H_{a'}$, $H_{b'}$, $H_{c'}$) of PPDO, respectively. In addition, the $-CH_3$ proton of ethoxy group had a characteristic peak around 1.2 ppm and the protons including the glucose unit and the $-CH_2$ of ethoxy group appeared at 3.1–5.2 ppm, which belonged to the substrate of EC. Above the peak assignments, the microstructure of EGP can be analyzed in detail through calculations with the peak intensity in ^{1}H NMR spectra. The values of *DP*, *DS*, *MS*, W_{PPDO}, and M_n can be estimated by Eqs. (1)–(5), respectively.

$$DP = \frac{(I_c + I_{c'})}{I_{c'}} \tag{1}$$

$$DS = \frac{2.17 \times 3 \times I_{c'}}{2 \times I_e} \tag{2}$$

$$MS = \frac{2.41 \times 3 \times (I_c + I_{c'})}{2 \times I_7} \tag{3}$$

$$W_{PPDO} = \frac{102 \times MS}{259.7 + 102MS} \tag{4}$$

$$M_n = 53{,}809 + DS \times DP \times 110 \times 102 \tag{5}$$

where *DP*, *DS*, *MS*, W_{PPDO}, and M_n delegated the degree of polymerization of PPDO (*DP*), the degree of substitution of copolymer (*DS*), the molar of substitution of copolymer (*MS*), the weight content of PPDO side-chains (W_{PPDO}) and the number average molecular weight of copolymers (M_n), respectively. Further, 2.17 denotes the ethoxy substitution of EC, I_e is the integral peak area of methyl group of ethyl cellulose, 102 g mol^{-1} is the molecular weight of PDO monomer, and 259.7 g mol^{-1} is the molecular weight of EC repeating unit.

3.2. Analysis of the reactivity of the graft polymerization

In order to investigate the effect of catalyst content on the structure parameters of EGPs, a series of copolymerization was carried out in which the molar ratio of EC and PDO was fixed at 1:15, the reaction temperature was 120 °C and the reaction time was 45 min. Fig. 2A showed the variations of *DP*, *DS*, and *MS* values of the products as a function of the different amount of catalyst. From the plots, we found that *DS*, *MS*, and *DP* almost progressively increased with the increment of catalyst in the range from 0.02 to 1.8 wt% (based on PDO monomer). It indicated that the substitution of the residual hydroxyls of the EC backbone took place more easily within this content range, owing to the rapid augment of the propagating centers. As we know, as the selective catalyst in the reaction, $Sn(Oct_2)$ may act as an assistant catalyst which co-initiates the ROP with the hydroxyl groups in the polymerization process (Gupta & Sahoo, 2001). Therefore, the amount of catalyst had a direct influence on the rate of the polymerization. When it was beyond 1.8 wt%, the values of *DS* and *MS* were almost invariant. At the same time, the *DP* value decreased obviously when $Sn(Oct)_2$ content was increased to 2.5 wt%. Further increased catalyst content, the *DP* values just kept the slight decrease. This indicated that the excessive amount of $Sn(Oct)_2$ was not beneficial for graft copolymerization and PPDO homopolymer may be produced easily which was irritated by the little water in the reaction system.

Fig. 2B depicts that the changing behaviors of *DP*, *DS*, and *MS* values with a lapse of reaction time at the fixed catalyst and reaction temperature ($Sn(Oct)_2$ content: 1 wt% based on PDO, reaction temperature: 120 °C). We can see clearly that at the earlier stage of the graft reaction the values of *DS*, *MS*, and *DP* increased monotonically within 15–60 min. This phenomenon meant that the active hydroxyl groups of the EC backbone can play a role as the propagating centers to initiate the grafting easily. However, the *DP*s of the PPDO side-chains decreased rapidly when 120 min was elapsed, and then it gradually decreased while the reaction time was further increased. As far as the *DS* was concerned, it was almost changeless in the practical time reaction scale from 60 to 180 min. The results indicated that, in the latter period of the reaction, the prolongation of reaction time made the new generating side-chains shorter and the promotion of *DS* more slow, owing to some side reaction such as the chain-transferring reaction and the inter-molecular or intra-molecular transesterification (Chen et al., 2008).

Fig. 2C exhibited the effect of different reaction temperatures on the values of *DP*, *DS*, and *MS* ($Sn(Oct)_2$ content:1 wt% based on PDO, reaction time:45 min). It was found that *DP* and *MS* slightly increased in the earlier stage from 100 to 120 °C. Both *DP* and *MS* arrived the maximum at 130 °C, whereas, decreased greatly above this temperature. On the other hand, compared with that of *DP* and *MS*, the *DS* appeared to plateau in the whole range of reaction temperature. It was well known that the ROP of PDO was in the thermodynamic equilibrium (Nishida et al., 2000), and the higher reaction temperature was helpful to enhance the copolymerization rate until the reaction converged to equilibrium with the gradual consumption of the PDO monomer. However, when the reaction temperature was too high to break the equilibrium, the thermal depolymerization of the grafted chains took place more easily.

To obtain EC-*g*-PPDOs with the different PPDO side-chains, an insight was provided into the copolymerization reaction with the variation of the in-feed molar ratio of EC/PDO in bulk under the optimal reaction conditions. The structure parameters and molecular weight of the graft copolymer synthesized with different feed ratio of PDO and EC were summarized in Table 1. It was found that both *MS* and W_{PPDO} values of graft copolymers almost increased in proportion to the amount of PDO monomer in-fed. And the compositional parameters of PPDO side-chains such as *DP* and *DS* also showed the same trend with the decrease of the in-feed molar ratio of EC/PDO. Accordingly, in this work, it indicated that the variation of the in-feed molar ratio of EC/PDO had an important influence on the compositional parameters of EGP copolymers. Moreover, GPC chromatograms demonstrated that the polydispersity (M_w/M_n) decreased monotonically from 2.01 to 1.56 accompanying by the progressive increment of the grafting chains. Theoretically, we can control the synthesis of the graft copolymers with different molecular structures of PPDO side-chains by changing the in-feed amount of EC/PDO in the bulk copolymerization.

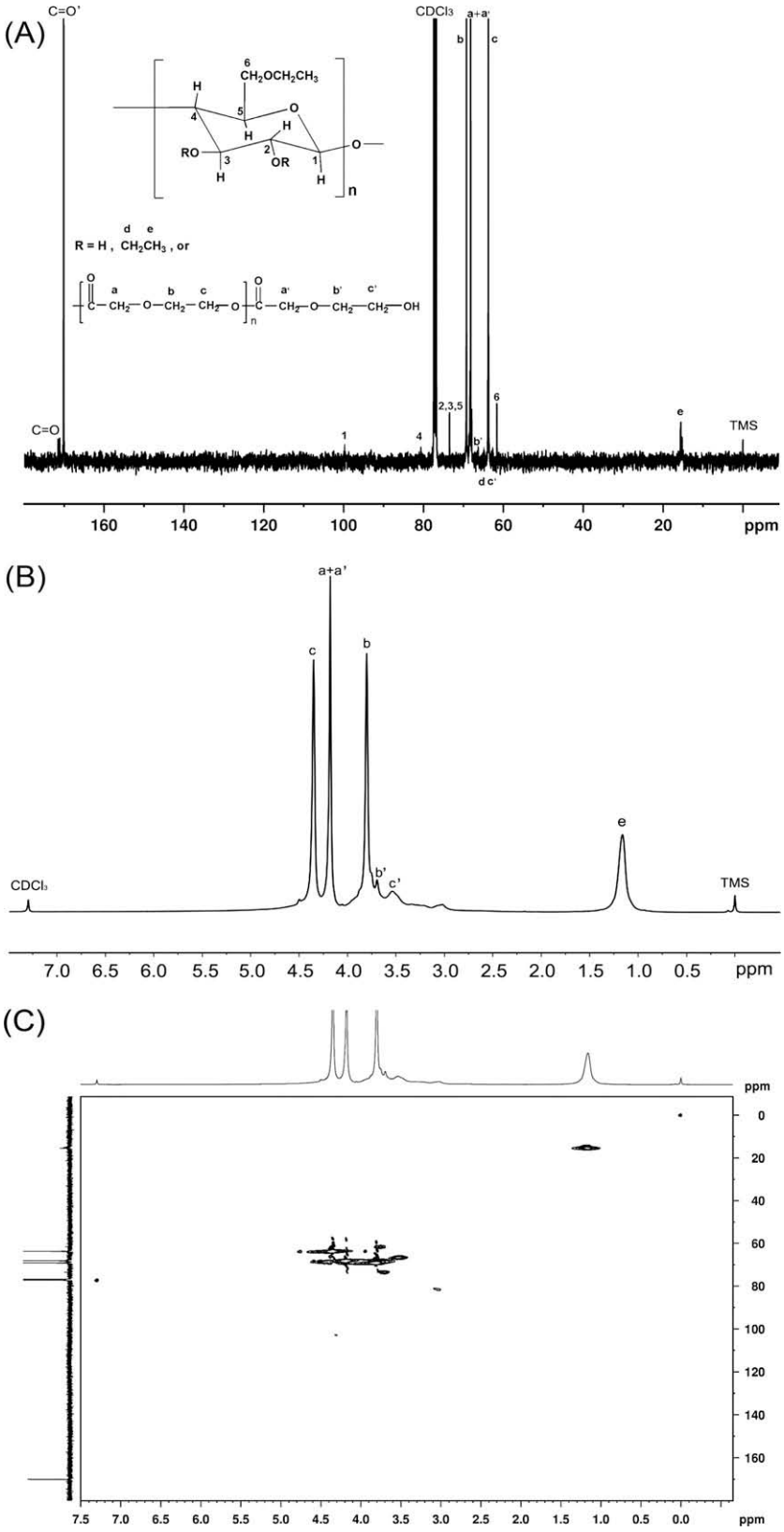

Fig. 1. Typical ^{13}C NMR (A), ^{1}H NMR (B), and HSQC (C) spectra of EC-*g*-PPDO copolymer.

3.3. Thermal transition behavior of EGP copolymers

As we know, the graft polymers will endow their substrates with different thermal properties due to their molecular architecture. Fig. 3A exhibits the cooling scans of EGP with different PPDO lengths after erasing thermal history at 120 °C for 5 min. Subsequently heating curves of EGP are shown in Fig. 3B. PPDO homopolymer used as a contrast for thermal analysis was synthesized

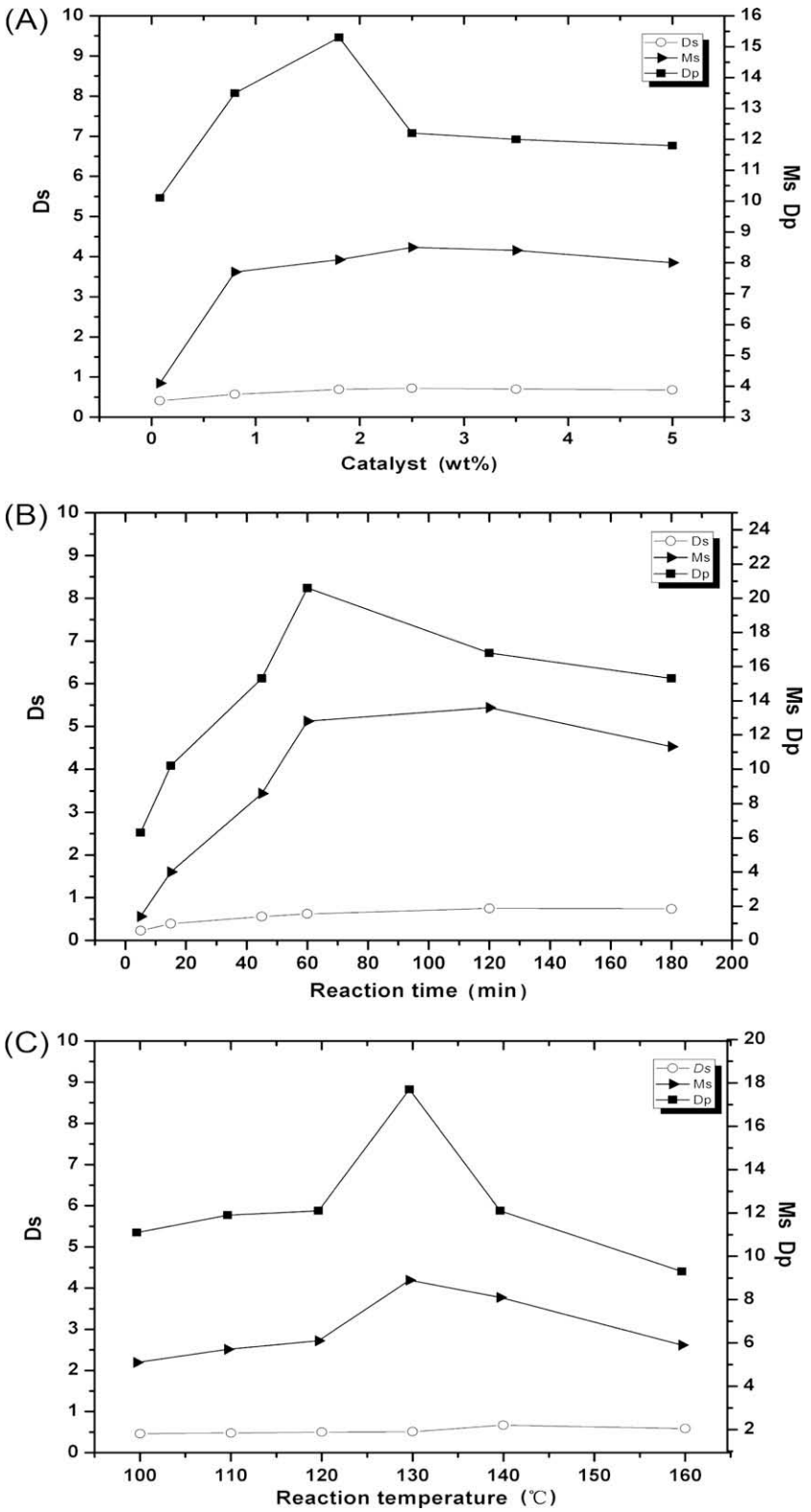

Fig. 2. (A) Effect of catalyst concentration on *DP*, *DS*, and *MS* of EGP copolymer (EC/PDO = 1:15 (mol/mol), 120 °C, 45 min); (B) effect of reaction time on *DP*, *DS*, and *MS* of EGP copolymer (EC/PDO = 1:15 (mol/mol), 1 wt%, 120 °C); (C) effect of reaction temperature on *DP*, *DS*, and *MS* of EGP copolymer (EC/PDO = 1:15 (mol/mol), 1 wt%; 45 min).

in the presence of $Sn(Oct)_2$ according to the reference (Nishida et al., 2000), whose viscosity-average molecular weight was 1.98. The data of all selective graft polymers and neat PPDO determined from Fig. 3 are listed in Table 2.

From the cooling curves, one can see clearly that no crystallization peak was found for EGP1 and EGP2 at a cooling rate of 10 °C min^{-1}, however, a distinct crystallization peak was observed for EGP3–EGP6, whose temperature of crystallization (T_c) increased with the growth of side-chains from 53.3 to 70.4 °C. Therefore, it can be indicatory that the crystalline ability of the graft copolymer was influenced greatly by its structure. Both EGP1 and EGP2 had the poor crystallization ability due to the shortness of side-chain

Table 1
The structure parameters of synthesized EGP copolymers.[a]

Sample	EC:PDO (mol:mol)	MS[b]	Db[a]	DS[b]	W_{PPDO}[b] (%)	$M_{n,NMR}$[b] ($\times 10^5$)	PPDO $M_{n,NMR}$[b] ($\times 10^5$)	$M_w/M_{n,GPC}$[c]
EGP1	1:5	2.5	6.5	0.39	49.5	1.07	0.53	2.01
EGP2	1:10	4.6	10.3	0.45	64.4	1.51	0.97	1.97
EGP3	1:15	6.1	12.1	0.50	70.5	1.83	1.29	1.92
EGP4	1:20	11.1	21.0	0.53	81.4	2.88	2.34	1.88
EGP5	1:30	17.9	22.1	0.82	87.6	4.32	3.78	1.74
EGP6	1:60	25.8	34.3	0.75	91.0	5.99	5.45	1.56

[a] Reaction conditions: 130 °C, 1 h, 1.8 wt% $Sn(Oct)_2$ based on PDO.
[b] Determined by ^1H NMR.
[c] Determined by GPC.

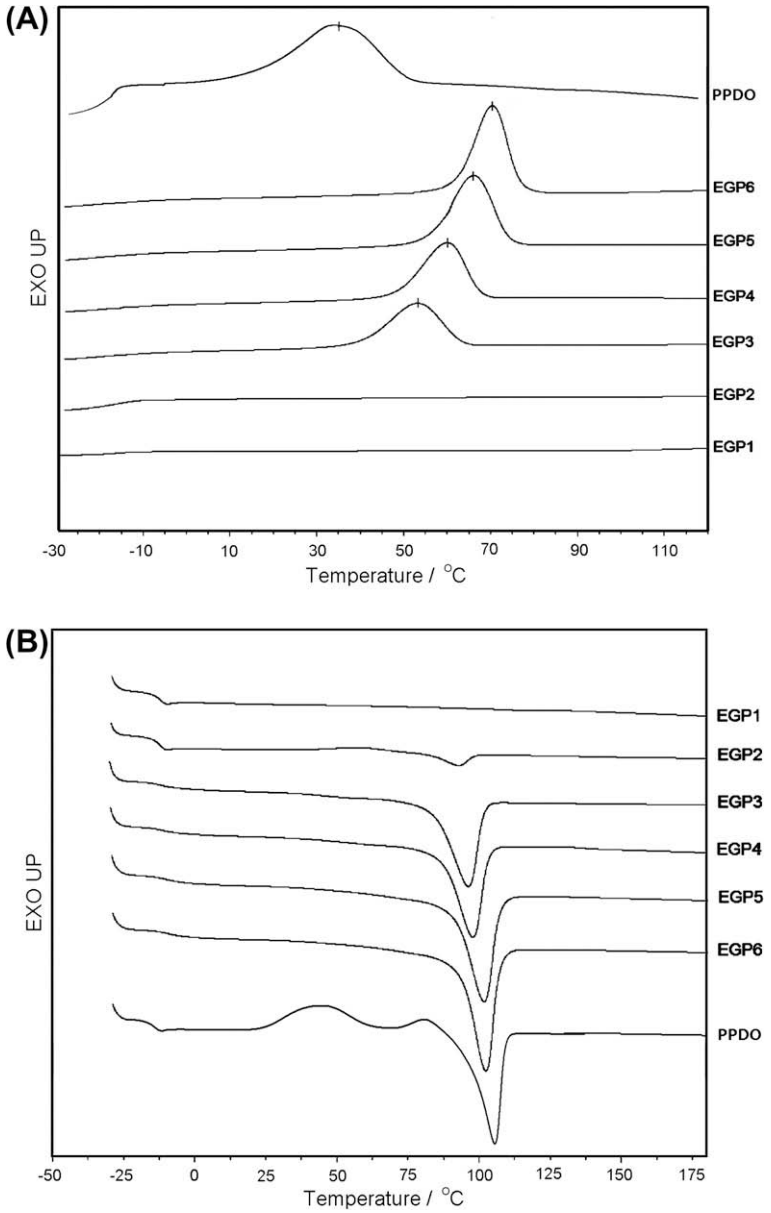

Fig. 3. DSC curves of EGP copolymers and PPDO in the first cooling run (A) and the second heating scan (B).

length. However, with the increment of PPDO content in the graft polymers, the length of PPDO side-chains was long enough to complete the copolymer crystallization during the cooling scan. Additionally, as far as we know, the copolymers with the narrower molecular distribution were also more prone to crystallize than their broad distribution counterparts. (The data of M_w/M_n of samples is listed in Table 1.)

Moreover, it is well known that both the glass transition temperature (T_g) and the crystalline melting temperature (T_m) are the crucial characteristic of any synthetic polymer, importantly influencing the polymer properties. Through the comparison of the DSC curves of copolymers (see Fig. 3B), one can behold that the thermal properties (T_g and T_m) of EGP copolymers were different from their substrate counterparts in the second heating scan. Because of

Table 2
Thermal properties of EC-*g*-PPDO copolymer and PPDO.

Sample	Cooling			Heating			T_{onset} (°C)	T_{max1} (°C)	T_{max2} (°C)
	T_c (°C)	ΔH_c (J/g)	T_g (°C)	T_m (°C)	ΔH_m (J/g)	X_c[a] (%)			
EC	–	–	–	–	–	–	337	356	–
EGP1	–	–	−11.8	–	–	–	168	253	352
EGP2	–	–	−12.0	92.7	5.6	6.2	–	–	–
EGP3	52.9	−34.0	−12.3	96.2	36.2	36.3	–	–	–
EGP4	59.9	−43.2	−11.1	97.8	44.6	38.8	–	–	–
EGP5	66.1	−50.8	−10.0	101.7	51.7	41.0	171	277	345
EGP6	70.4	−57.6	−9.4	102.3	58.3	44.7	–	–	–
PPDO	38.9	−58.3	−10.2	108.7	76.3	53.9	–	–	–

[a] $\chi_c = \frac{\Delta H_m}{\Delta H_m^0 \times \text{PPDO}\ (\text{wt\%})}$; ΔH_m^0 denoted the heat of melting using the melting of 141.3 J/g of 100% crystalline PPDO.

the complete crystallization of EGP3–EGP6 samples in the cooling run, their melting temperatures (T_m) were clearly found from the heating scans. However, in this case, for the graft polymers (EGP1 and EGP2) with the poor crystallization ability, no melting points were found. This phenomenon could be ascribed to the fact that imperfect crystals may form more perfect crystals at higher temperature before melting, just like to linear PPDO and PBS (Teramoto & Nishio, 2003). And the T_m of EGP1 can almost invisible in the second heating curve. Moreover, from the results of the melting point of EGPs (exhibited in Table 2), one can see that the T_ms of copolymers was closely related to the microstructure of PPDO side-chains. That is, the higher the *DP* and *DS* of the graft polymers, the higher the melting temperature and melting enthalpy.

On the other hand, as far as the T_gs of copolymers were concerned, the data of T_gs in Table 2 disclosed that a clear and sharp decrease of the T_g (138.9 °C) of EC (Lara, Mariastella, & Patrizia, 1998) to the lower temperature, which was close to the T_g of PPDO homopolymer (−10.2 °C). For example, when 49.5 wt% PPDO (EGP1) was introduced onto the backbone of EC, the corresponding T_g was −11.8 °C. And while the content of PPDO side-chain was 64.4 wt%, the counterpart of sample (EGP2) fell to −12.0 °C. In this case, it illuminated that the PPDO side-chains could play an effective role as the 'internal' plasticizer, just like other semi-rigid cellulosic materials grafted with aliphatic polyesters such as PLA (Teramoto & Nishio, 2003). In addition, the T_g of EGP3 (W_{PPDO} = 70.4 wt%) exhibited a minimum of −12.3 °C, and with further increase PPDO content, the T_gs of the graft polymers appeared to increase slightly (see in Table 2). For instance, for EGP5, whose W_{PPDO} was 87.6 wt%, its T_g was −10.0 °C higher than that of EGP3. As we know, for the crystalline polymer, it is the fact that the molecular motion in amorphous region is restricted by the crystalline region, such as polyethylene and polypropylene. From Table 2, we can see clearly that, for samples (EGP3–EGP6), their T_gs enhanced orderly with the elevation of their corresponding X_c. Also, it is difficult to detect the glass transition temperatures (T_gs) of samples (EGP3–EGP6) with the high crystallinity by DSC, compared with EGP1 and EGP2.

3.4. Thermal stability of EGP copolymers

The thermal stability of copolymer was examined by TG in N_2 atmosphere at a heating rate of 10 °C min^{-1}. All relevant results based on the TG and DTG curves are summarized in Table 2. Obviously, one can behold from the data that neat EC exhibited only one maximal decomposition temperature corresponding to 356 °C. However, in contrast with EC substrate, both EGP1 and EGP5 manifested two maximum decomposition temperatures (T_{max}), in which T_{max1} was ascribed to the decomposition of PPDO, and T_{max2} was assigned to the counterpart of EC.

From Table 2, it can be found that the thermal stability of EC substrate was better than that of copolymers, based on the fact that the maximum decomposition temperature (T_{max2}) of EGP were lower than that of pure EC. For example, T_{max2} of EGP1 and EGP5 were 352 and 345 °C, respectively, compared with the T_{max} of EC (356 °C). This could be ascribed to the farther breakage of the residual hydrogen bonds in the original structure of EC after grafting PPDO chains (Liu et al., 2008). Furthermore, we can see that the structure of copolymers had a significant effect on the stability of EGP. EGP1 with the shortest PPDO chains started to decompose at 168.1 °C, while EGP5 with longer PPDO chains had a higher initial decomposition temperature (170.6 °C). As far as T_{max1} of EGP was concerned (see in Table 2), the similar trend was observed, namely, the longer the PPDO chains, the better the thermal stability of graft copolymers.

3.5. Crystal morphology of the graft copolymers

The spherulitic morphology of EGPs and PPDO were investigated by the polarizing optical microscope (POM) at 70 °C. The relevant POMs of the selective samples are shown in Fig. 4. PPDO exhibited well defined Maltese crosses and banded spherulites at 70 °C which had been well discussed by Sabino, Feijoo, and Muller (2000). In contrast with the spherulitic image of PPDO, the spherulites of graft copolymers were imperfect. Beside this, the spherulitic growth of the graft copolymers was slower than that of PPDO. As far as EGP1 with lower W_{PPDO} (W_{PPDO} = 49.5%) was concerned, its spherulites can almost not be observed at 70 °C until a lapse of 15 min. However, for EGP3 and EGP5 with higher W_{PPDO}, only 5 and 3 min were needed to observe the spherulites, respectively. These indicated that the composition of the graft copolymers affects the crystallization process, which was in accordance with the DSC result. In this case, at least, it can be said that after the graft copolymerization, the semi-rigid backbones of EC prevented the motion of PPDO side-chains, due to the existence of the EC segment in graft copolymers. Therefore, the spherulite growth rates of EGP with higher W_{PPDO} were faster than the lower W_{PPDO} counterpart.

3.6. Crystallization structure of EGP copolymers

The WAXD patterns of neat EC, PPDO, EGP1, EGP3, and EGP5 are shown in Fig. 5. All samples were pretreated at 40 °C for 48 h before measuring. From the patterns of EC, two characteristic broad reflection peaks appeared at 2θ = 7.4° and 20.9°, respectively. However, as for EGPs, against their substrate counterparts, the reflection peak at 7.4° disappeared gradually with the increase of W_{PPDO} in copolymers. Besides these, some new sharp peaks were found at 2θ = 21.7°, 22.9°, and 28.4°, which accords with those of PPDO crystallization reflection peaks. And the more the W_{PPDO} in copolymers the higher the crystallization outline for the selective samples (EGP1, EGP3, and EGP5). Accordingly, it indicated that

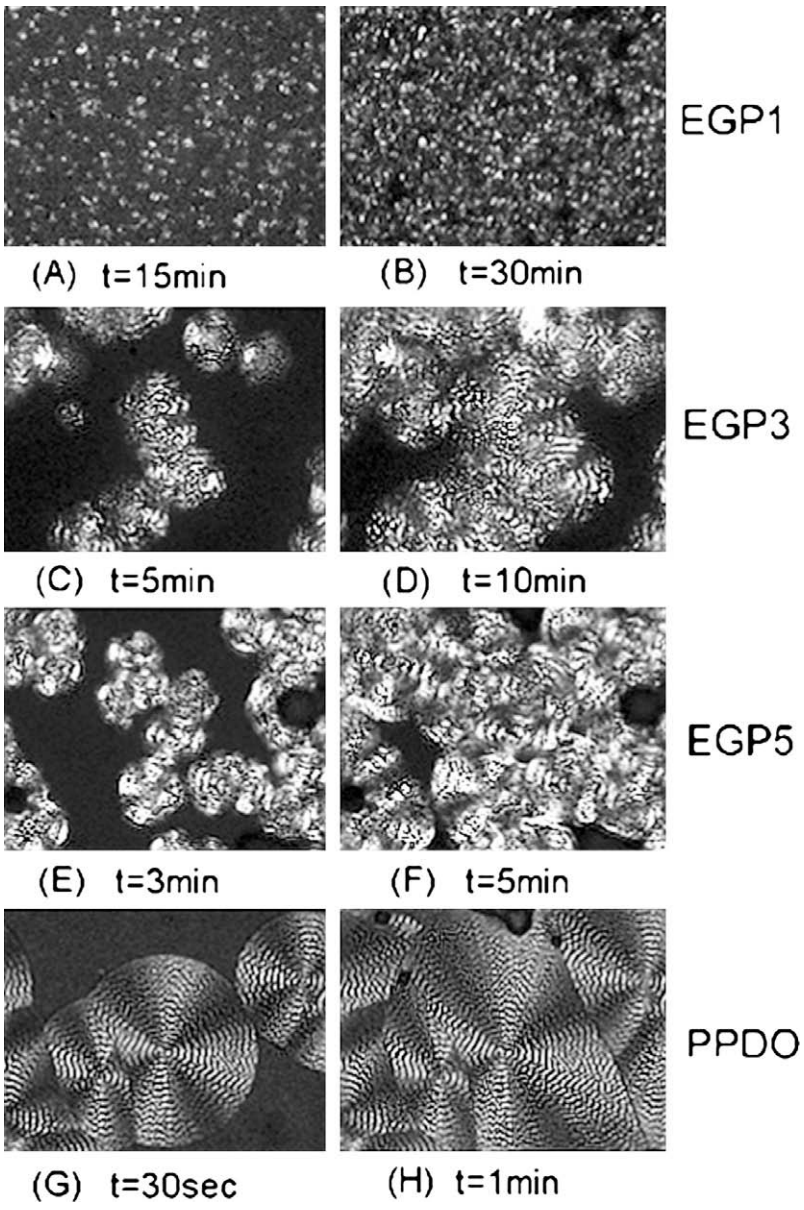

Fig. 4. POM photos of PPDO and EGP copolymers.

the introduction of PPDO onto EC backbone could destroy the original crystallization pattern of EC, and samples with the longer PPDO side-chains were easily prone to crystalline, as compared with the shorter side-chains ones.

3.7. In vitro degradation behaviors of PPDO and EGP copolymers

The in vitro degradation behavior of PPDO and EGP copolymers are shown in Fig. 6. One can see that the degradation rate of neat PPDO was very slow. After 30 days, the weight loss of PPDO was only 6.8%. As we know, the crystallinity is one of the important factors for the degradation of EGP copolymers contributing to degradability of PPDO segment by random hydrolytic ester bond cleavage (Kenji, Masakazu, & Yoshito, 2001). Compared with the linear PPDO, EGP copolymers was a polymer with lower crystallinity. Thus, it is reasonable that the degradation rate of copolymers were faster than that of neat PPDO. Furthermore, the degradation rate of EGP sample with lower X_c was easier than that of higher X_c counterpart. As far as EGP5 (X_c = 41.0%) was concerned, the weight loss was just 8.2% after degradation for 30 days, however, it was 9.9% for EGP3 (X_c = 36.3%). For EGP1 with the poor crystallinity, the degradation rate was 14.1%. In this work, at least, it can be explained that the increasing crystallinity in copolymers prevents water molecule from penetrating into amorphous regions of graft copolymers, resulting in a deceleration of the cleavage of PPDO side-chains.

4. Conclusions

A novel biodegradable copolymer (EGP) was successfully synthesized via the ring-opening graft copolymerization of ρ-dioxanone (PDO) with a tin 2-ethylhexanoate ($Sn(Oct)_2$) catalyst in bulk at 120 °C. Through changing the molar ratios of PDO monomer to EC, PPDO side-chains with the different lengths can be introduced onto EC backbone. EGP resultants showed the single T_gs which was sharply decreased from the 138.9 °C of EC substrate, close to that of linear PPDO. And the values of T_m and X_c of EGPs were increased with the increment of the length of PPDO. Further-

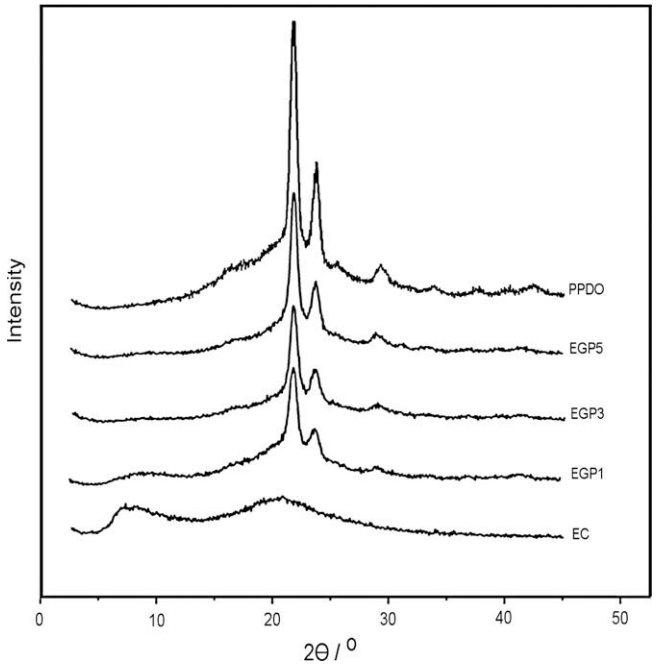

Fig. 5. WAXD profiles of EC, PPDO, and EGP copolymers.

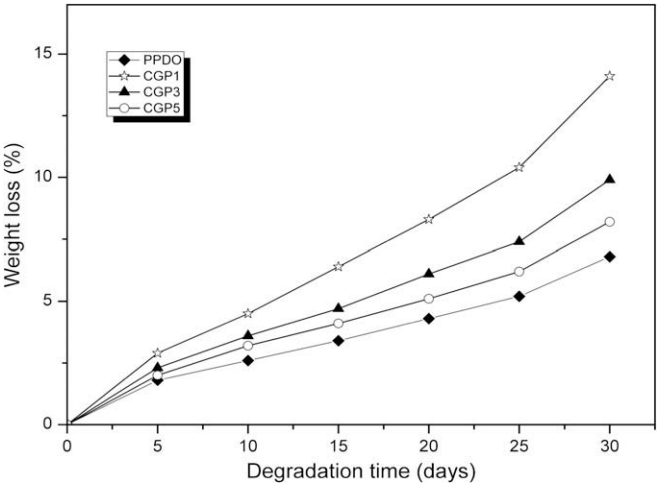

Fig. 6. The in vitro degradation behaviors of PPDO and EGP copolymers.

more, the thermal stability of EGPs with short PPDO branches was poorer than that of EGPs with long PPDO side-chains. Moreover, EGP copolymers also revealed crystalline properties that were different from that of linear PPDO. The in vitro degradation rate of EC-*g*-PPDO was faster than that of linear PPDO due to the poorer crystallinity of PPDO branches.

Acknowledgements

This work was supported financially by the National Science Fund for Distinguished Young Scholars (50525309), and the National Science Foundation of China (20974066) as well as the Program for New Century Excellent Talents in University (NCET-06-0791). The authors also acknowledge the Analytical & Testing Center of Sichuan University for the NMR measurements.

References

Bisht, K. S., Deng, F., Gross, R. A., Kaplan, D. L., & Swift, G. (1998). Ethyl glucoside as a multifunctional initiator for enzyme-catalyzed regioselective lactone ring-opening polymerization. *Journal of the American Chemical Society, 120*(7), 1363–1367.

Brostrom, J., Boss, A., & Chronakis, I. S. (2004). Biodegradable films of partly branched poly(L-lactide)-co-poly(ε-caprolactone) copolymer: Modulation of phase morphology, plasticization properties and thermal depolymerization. *Biomacromolecules, 5*(3), 1124–1134.

Chen, S. C., Wang, X. L., Wang, Y. Z., Yang, K. K., Zhou, Z. X., & Wu, G. (2007). In vitro degradation of biodegradable blending materials based on poly(ρ-dioxanone) and poly(vinyl alcohol)-graft-poly(ρ-dioxanone) with high molecular weights. *Journal of Biomedical Materials Research Part A, 80A*(2), 453–465.

Chen, Y. Y., Wu, G., Qiu, Z. C., Wang, X. L., Zhang, Y., Lu, F., et al. (2008). Microwave-assisted ring-opening polymerization of ρ-dioxanone. *Journal of Polymer Science Part A: Polymer Chemistry, 46*(10), 3207–3213.

Chen, S. C., Zhou, Z. X., Wang, Y. Z., Wang, X. L., & Yang, K. K. (2006). A novel biodegradable poly(ρ-dioxanone)-grafted poly(vinyl alcohol) copolymer with a controllable in vitro degradation. *Polymer, 47*(1), 32–36.

Deng, C., Rong, G., Tian, H., Tang, Z., Chen, X., & Jing, X. (2005). Synthesis and characterization of poly(ethylene glycol)-b-poly (L-lactide)-b-poly(L-glutamic acid) triblock copolymer. *Polymer, 46*(3), 653–659.

Gan, Z., Yu, D., Zhong, Z., Liang, Q., & Jing, X. (1999). Enzymatic degradation of poly(ε-caprolactone)/poly(DL-lactide) blends in phosphate buffer solution. *Polymer, 40*(10), 2859–2862.

Gupta, K. C., & Sahoo, S. (2001). Graft copolymerization of acrylonitrile and ethyl methacrylate comonomers on cellulose using ceric ions. *Biomacromolecules, 2*(1), 239–247.

Haruo, N., Mitsuhiro, Y., Masumi, N., Takeshi, E., & Yutaka, T. (2000). Synthesis of metal-free poly(1,4-dioxan-2-one) by enzyme-catalyzed ring-opening polymerization. *Journal of Polymer Science Part A: Polymer Chemistry, 38*(9), 1560–1567.

Ho, M. H., Tu, C. Y., Hsieh, H. J., Lai, J. Y., Chen, W. J., & Wang, D. M. (2006). Promotion of cell affinity of porous PLLA scaffolds by immobilization of RGD peptides via plasma treatment. *Macromolecular Bioscience, 6*(1), 90–98.

Kenji, T., Masakazu, S., & Yoshito, I. (2001). The pH dependence of monofilament sutures on hydrolytic degradation. *Journal of Biomedical Materials Research, 58*(5), 511–518.

Ko, B. T., & Lin, C. C. (2001). Synthesis, characterization, and catalysis of mixed-ligand lithium aggregates, excellent initiators for the ring-opening polymerization of L-lactide. *Journal of the American Chemical Society, 123*(33), 7973–7977.

Kowalski, A., Libiszowski, J., Biela, T., Cypryk, M., Duda, A., & Penczek, S. (2005). Kinetics and mechanism of cyclic esters polymerization initiated with tin(II) octoate. Polymerization of ε-caprolactone and L,L-lactide co-initiated with primary amines. *Macromolecules, 38*(20), 8170–8176.

Kricheldorf, H. R., & Damrau, D. O. (1998). Polylactones, 42. Zn L-lactate-catalyzed polymerizations of 1,4-dioxan-2-one. *Macromolecular Chemistry and Physics, 199*(6), 1089–1097.

Lara, F., Mariastella, S., & Patrizia, S. (1998). Biodegradation of blends of bacterial poly(3-hydroxybutyrate) with ethyl cellulose in activated sludge and in enzymatic solution. *Macromolecular Chemistry and Physics, 199*, 695–703.

Li, W. J., Danielson, K. G., Alexander, P. G., & Tuan, R. S. (2003). Biological response of chondrocytes cultured in threedimensional nanofibrous poly(ε-caprolactone) scaffolds. *Journal of Biomedical Materials Research Part A, 67*, 1105–1114.

Libiszowski, J., Kowalski, A., Szymanski, R., Duda, A., Raquez, J. M., Degee, P., et al. (2004). Monomer–linear macromolecules–cyclic oligomers equilibria in the polymerization of 1,4-dioxan-2-one. *Macromolecules, 37*(1), 52–59.

Liu, G. Y., Zhai, Y. L., Wang, X. L., Wang, W. T., Pan, Y. B., Dong, X. T., et al. (2008). Preparation, characterization, and in vitro drug release behavior of biodegradable chitosan-graft-poly(1,4-dioxan-2-one) copolymer. *Carbohydrate Polymers, 74*(4), 862–867.

Lonnberg, H., Zhou, Q., Brumer, H., Teeri, T. T., Malmstrom, E., & Hult, A. (2006). Grafting of cellulose fibers with poly(ε-caprolactone) and poly(L-lactic acid) via ring-opening polymerization. *Biomacromolecules, 7*(7), 2178–2185.

Meng, F., Zheng, S., Zhang, W., Li, H., & Liang, Q. (2006). Nanostructured thermosetting blends of epoxy resin and amphiphilic poly(ε-caprolactone)-block-polybutadiene-block-poly(ε-caprolactone) triblock copolymer. *Macromolecules, 39*(2), 711–719.

Nishida, H., Yamashita, M., Endo, T., & Tokiwa, Y. (2000). Equilibrium polymerization behavior of 1,4-dioxan-2-one in bulk. *Macromolecules, 33*(19), 6982–6986.

Odile, D. C., Blanca, M. V., & Didier, B. (2004). Controlled ring-opening polymerization of lactide and glycolide. *Chemical Reviews, 104*(12), 6147–6176.

O'Keefe, B. J., Monnier, S. M., Hillmyer, M. A., & Tolman, W. B. (2001). Rapid and controlled polymerization of lactide by structurally characterized ferric alkoxides. *Journal of the American Chemical Society, 123*(2), 339–340.

Raquez, J. M., Degee, P., Narayan, R., & Dubois, P. (2001). Some thermodynamic, kinetic, and mechanistic aspects of the ring-opening polymerization of 1,4-dioxan-2-one initiated by Al(OiPr)3 in bulk. *Macromolecules, 34*(24), 8419–8425.

Raquez, J. M., Narayan, R., & Dubois, P. (2000). "Coordination-insertion" ring-opening polymerization of 1,4-dioxan-2-one and controlled synthesis of diblock copolymers with ε-caprolactone. *Macromolecular Rapid Communications, 21*(15), 1063–1071.

Rieger, J., Coulembier, O., Dubois, P., Bernaerts, K. V., Du, F. E., Jerome, R., et al. (2005). Controlled synthesis of an ABC miktoarm star-shaped copolymer by sequential ring-opening polymerization of ethylene oxide, benzyl β-malolactonate, and ε-caprolactone. *Macromolecules, 38*(26), 10650–10657.

Sabino, M. A., Feijoo, J. L., & Muller, A. J. (2000). Crystallisation and morphology of poly(*p*-dioxanone). *Macromolecular Chemistry and Physics, 201*(18), 2687–2698.

Shen, D., & Huang, Y. (2004). The synthesis of CDA-g-PMMA copolymers through atom transfer radical polymerization. *Polymer, 45*(21), 7091–7097.

Shen, D., Yu, H., & Huang, Y. (2005). Densely grafting copolymers of ethyl cellulose through atom transfer radical polymerization. *Journal of Polymer Science Part A: Polymer Chemistry, 43*(18), 4099–4108.

Teramoto, Y., & Nishio, Y. (2003). Cellulose diacetate-graft-poly(lactic acid)s: Synthesis of wide-ranging compositions and their thermal and mechanical properties. *Polymer, 44*(9), 2701–2709.

Wang, F., Bronich, T. K., Kabanov, A. V., Rauh, R. D., & Roovers, J. (2005). Synthesis and evaluation of a star amphiphilic block copolymer from poly(ε-caprolactone) and poly(ethylene glycol) as a potential drug delivery carrier. *Bioconjugate Chemistry, 16*, 397–405.

Wang, C. H., & Hsiue, G. H. (2005). Polymer-DNA hybrid nanoparticles based on folate-polyethylenimine-block-poly(L-lactide). *Bioconjugate Chemistry, 16*(2), 391–396.

Wang, H., Qiu, K. Y., & Gu, Z. W. (1998). Synthesis of poly(1,4-dioxan-2-one-co-trimethylene carbonate) for application in drug delivery systems. *Journal of Polymer Science Part A: Polymer Chemistry, 36*(8), 1301–1307.

Wang, X. L., Yang, K. K., Wang, Y. Z., Zhou, Z. X., & Jin, Y. D. (2004). Synthesis and nuclear magnetic resonance analysis of starch-g-poly(1,4-dioxan-2-one) copolymers. *Journal of Polymer Science Part A: Polymer Chemistry, 42*(14), 3417–3422.

Yang, K. K., Wang, X. L., & Wang, Y. Z. (2002). Poly(*p*-dioxanone) and its copolymers. *Journal of Macromolecular Science – Polymer Reviews, C42*(3), 373–398.

Yuan, W., Yuan, J., Zhang, F., & Xie, X. (2007). Syntheses, characterization, and in vitro degradation of ethyl cellulose-graft-poly(ε-caprolactone)-block-poly(L-lactide) copolymers by sequential ring-opening polymerization. *Biomacromolecules, 8*(4), 1101–1108.

Zhu, J., Wang, W. T., Wang, X. L., Li, B., & Wang, Y. Z. (2009). Green synthesis of a novel biodegradable copolymer base on cellulose and poly(ρ-dioxanone) in ionic liquid. *Carbohydrate Polymers, 76*, 139–144.